

Fig S1: Androgen induced DNA DSBs are dependent on AR. (A,C) Quantitation of 53BP1 foci following exposure to R1881, 10 nM DHT and olaparib alone or in combination for 24 h in LNCaP, LNCaP^{AR} (B,D) Quantitation of 53BP1 foci following exposure to R1881, 10 nM DHT and olaparib alone or in combination for 24 h in PC3 and PC3^{AR} cells respectively. (E) Confocal immunostaining of γH2AX in PC3 and PC3^{AR} cells treated with different concentrations of R1881. (F,G,H) Quantitation of the kinetics of DNA damage by γH2AX foci/cell in LNCaP, LNCaP^{AR}, and PC3 and PC3^{AR} following 10 nM R1881 or DHT at intervals after treatment. (I,J) Graphs represent comet tail moment and length in LNCaP and LNCaP^{AR} cells following 10 nM R1881. In A-D, and F-I, data represent the mean ± SD; n=4 replicates per experiment; p≤0.05 (*), p<0.01 (**) by two-way ANOVA.

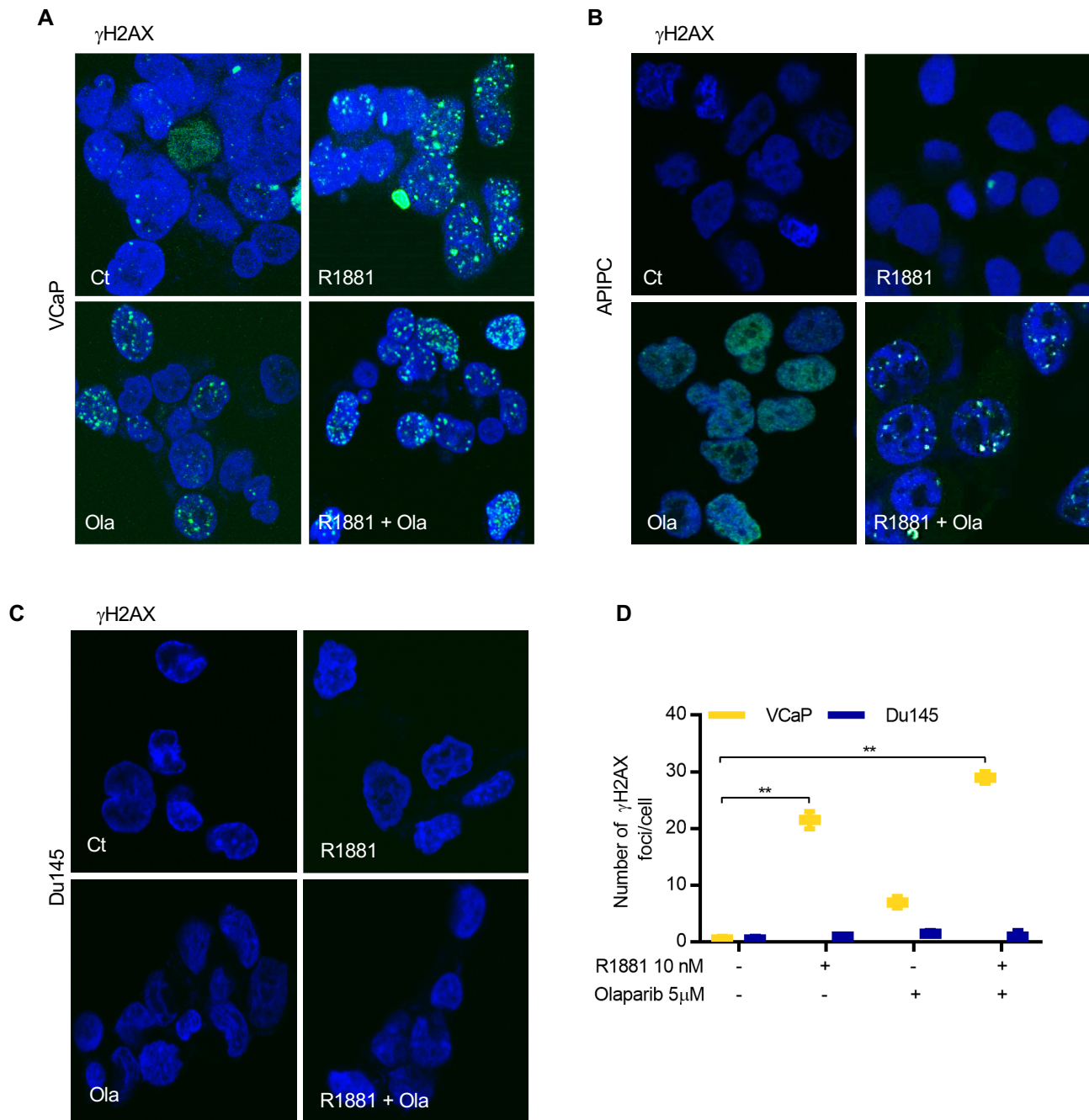


Fig S2: Assessments of DNA damage in AR negative and positive cells following SPA and Olaparib Treatment. (A,B,C) Confocal immunostaining of γ H2AX in VCaP, LNCaP^{APIPC} and Du145 cells treated with 10 nM R1881 and Olaparib (Ola) alone or in combination. (D) Graphical representation of γ H2AX in VCaP and Du145 cells treated with 10 nM R1881 and Olaparib alone or in combination. ** $p < 0.01$ by two-way ANOVA and $n = 3$ experimental replicates.

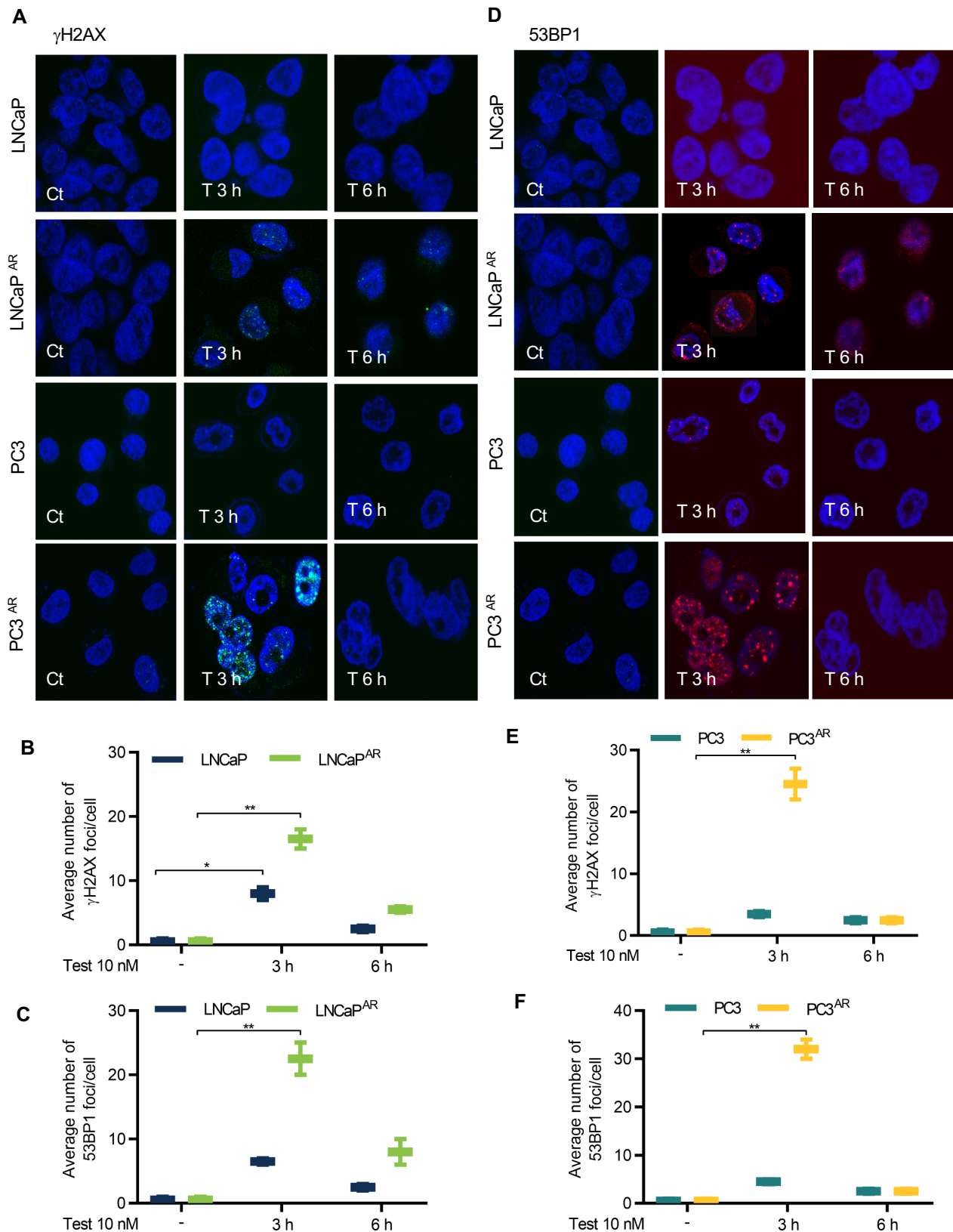


Fig S3: Kinetics of testosterone induced DNA DSBs. Confocal immunostaining (**A,D**) and graphical representation (**B,E**) of γ H2AX and (**C,F**) 53BP1 in LNCaP, LNCaP^{AR}, and PC3 and PC3^{AR} respectively following 10 nM testosterone exposure for 3 and 6h. In B,C,E,F data represent the mean \pm SD; n=4 replicates per experiment; $p \leq 0.05$ (*), $p < 0.01$ (**) by two-way ANOVA.

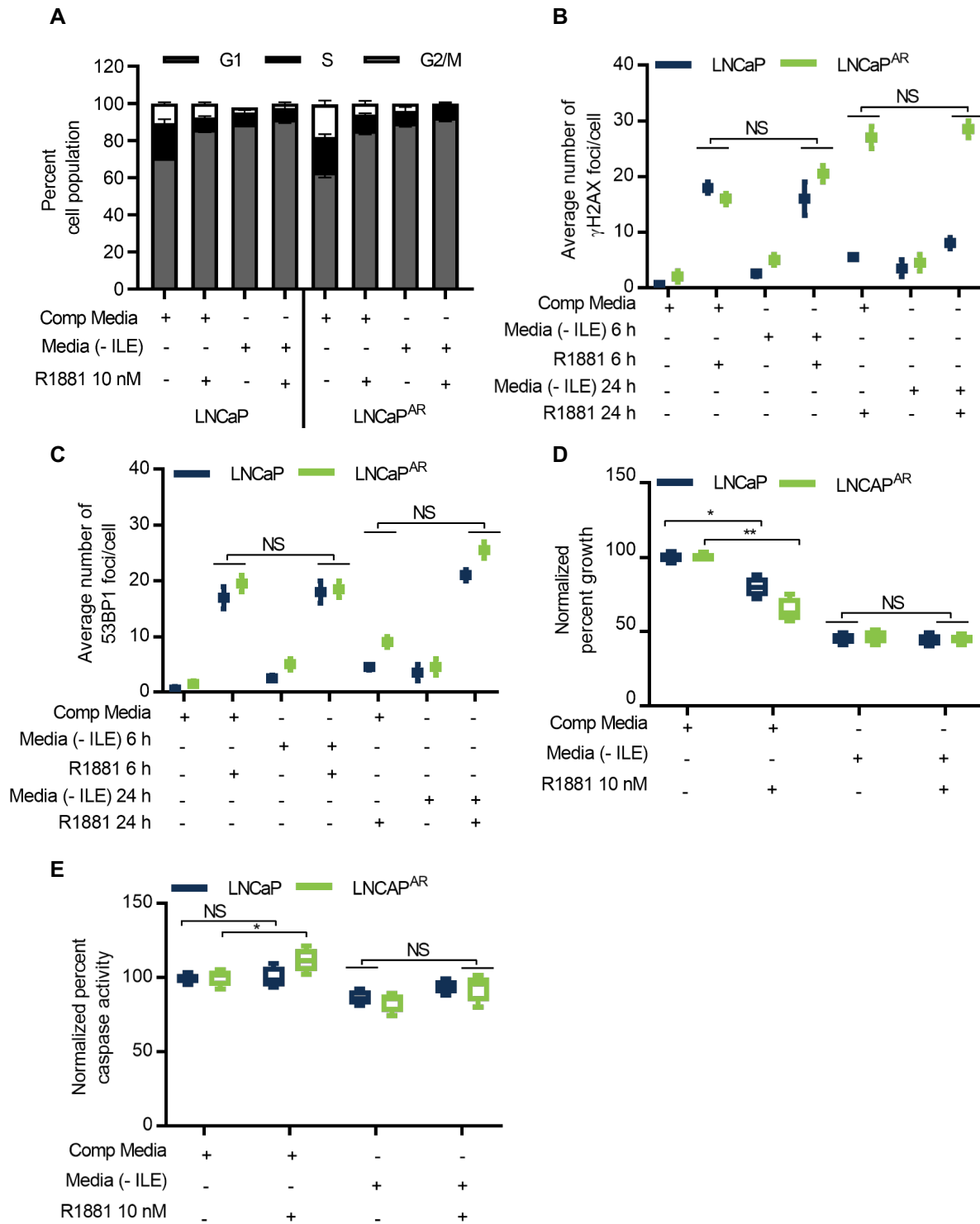


Fig S4: SPA induces DNA damage in quiescent prostate cancer cells. (A) Cell cycle analysis demonstrates the synchronizing effect of isoleucine starvation in both LNCaP and LNCaP^{AR} cells. (B,C) Graphical representation of γ H2AX and 53BP1 foci in LNCaP and LNCaP^{AR} cells following SPA treatment under isoleucine deprived condition (- ILE). (D,E) Percentage of cell growth and caspase activity was evaluated after 3 days of R1881 exposure under the isoleucine depleted conditions * $p \leq 0.05$, ** $p < 0.01$ by two way ANOVA and $n=4$ replicates.

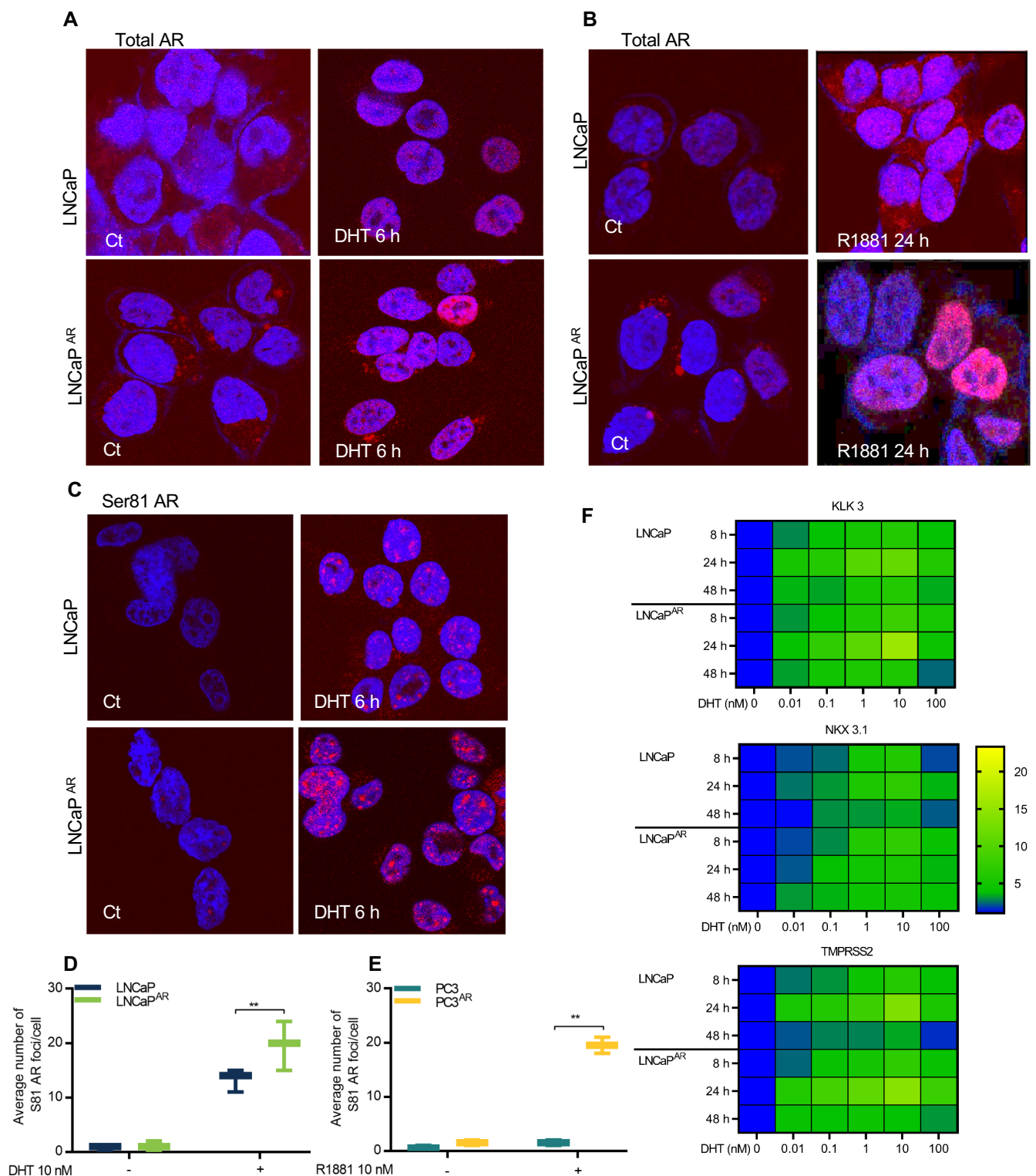


Fig S5: Effects of SPA on AR localization and function. Confocal immunostaining of total AR in LNCaP and LNCaP^{AR} cells following (A) 10 nM DHT and (B) 10 nM R1881. (C,D) Confocal immunostaining and graphical representation of Ser81 AR in LNCaP and LNCaP^{AR} cells following 10 nM DHT. (E) Quantitation of Ser81 AR foci in PC3 and PC3^{AR} after 24h of 10 nM R1881 treatment. (F) Transcript levels of KLK3, NKX3.1 and TMPRSS2 in LNCaP cells following exposure to DHT concentrations 0.01 to 100 nM. ** p<0.01 by two way ANOVA and n=4 replicates.

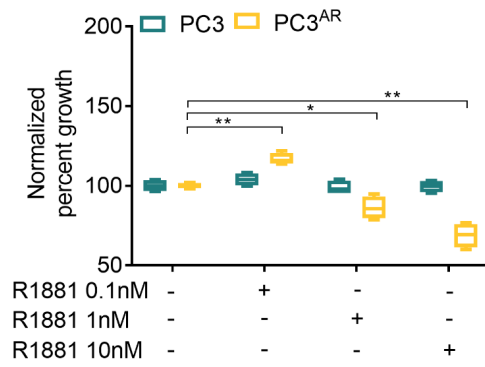
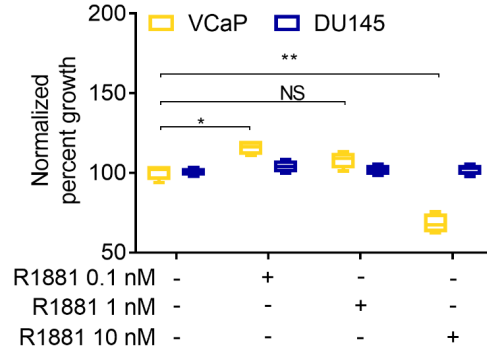
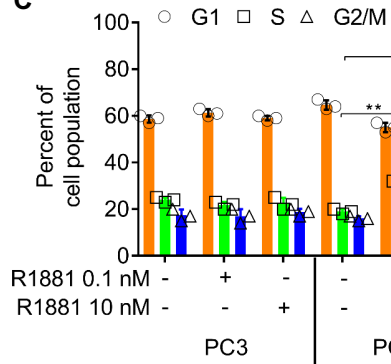
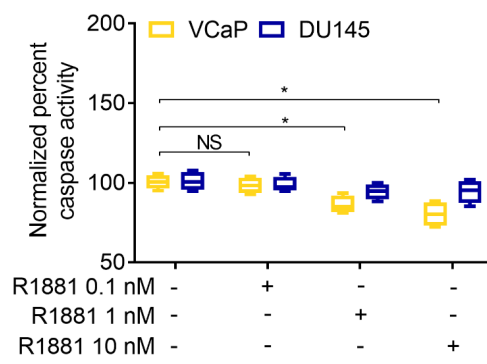
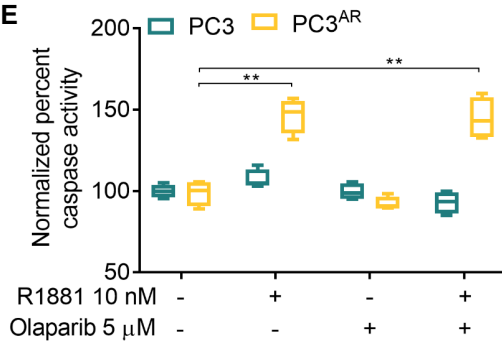
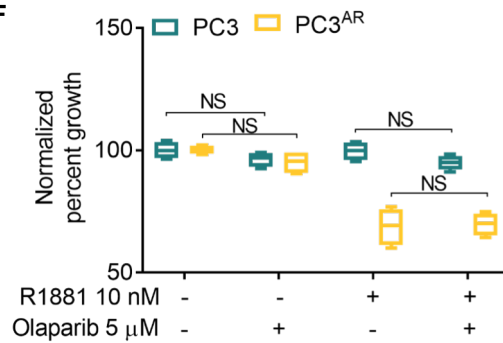
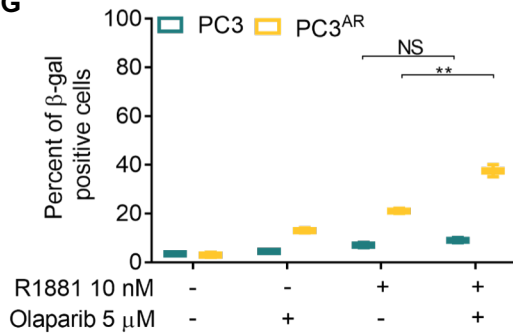
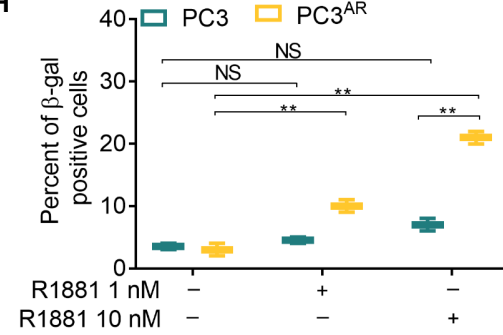
A**B****C****D****E****F****G****H**

Fig S6: Effects of SPA and PARP inhibition on prostate cancer cell proliferation, apoptosis and senescence. (A,B) Effects of androgen concentrations on the growth of PC3, PC3^{AR} VCaP and DU145 cells after 3 days. (C) Cell cycle profile for PC3 and PC3^{AR} following different concentrations of R1881 for 3 days. (D, E) Quantitation of apoptosis by caspase activity in VCaP and Du145 and PC3 and PC3^{AR} cells following exposure to R1881 and Olaparib for 3 days. (F,G,H) Quantitation of cell growth and senescence by senescence-associated beta-galactosidase staining. The percentage of senescent cells is shown after 3 days treatment of different doses of R1881 and olaparib in PC3 and PC3^{AR} cells. Data represent the mean \pm SD; n=4 replicates per experiment; $p \leq 0.05$ (*), $p < 0.01$ (**) by two-way ANOVA.

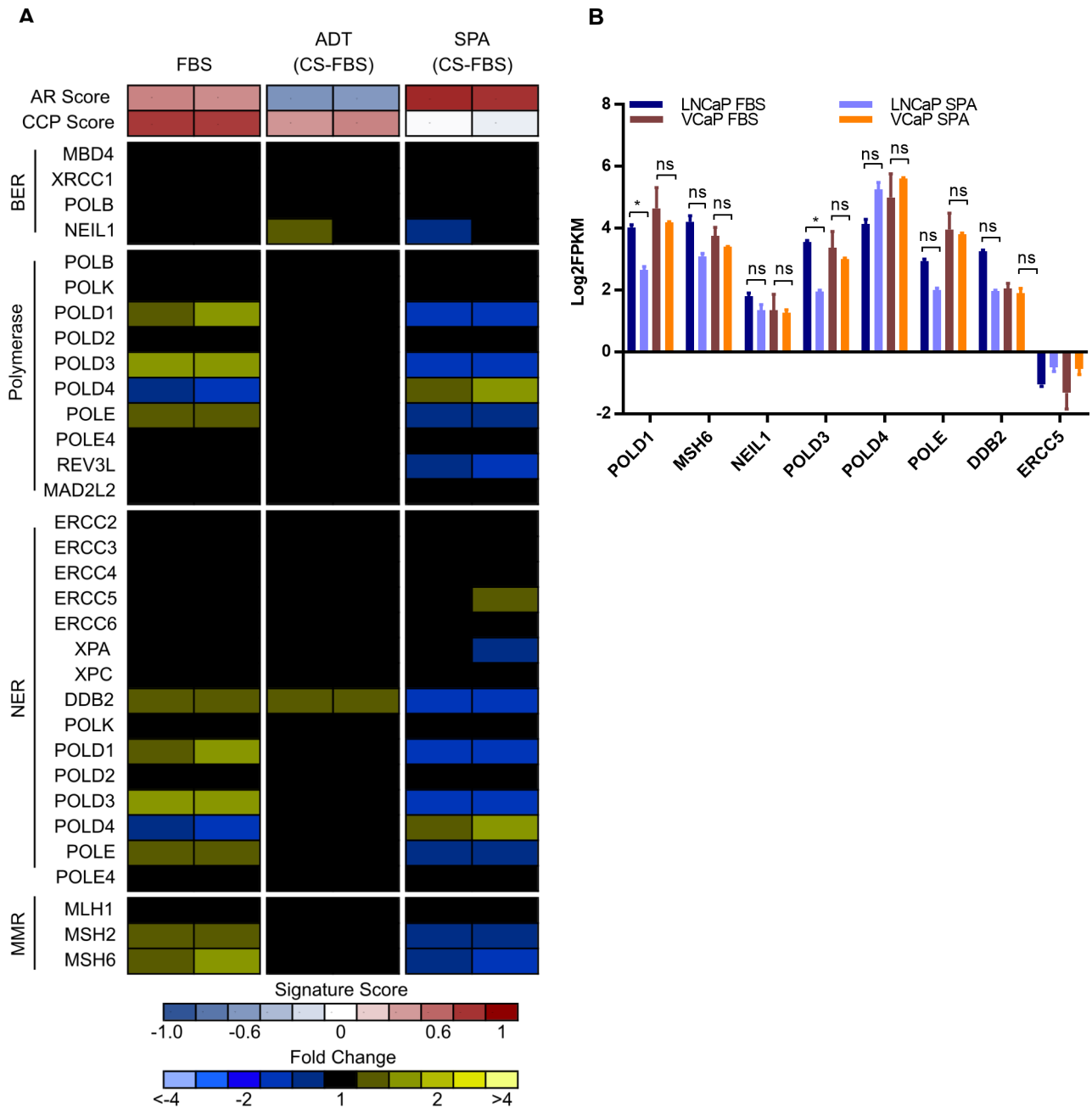


Fig S7. Involvement of other repair pathways such as BER, NER and MMR along with polymerases, in LNCaP cells following SPA treatment. **A.** Transcript levels of BER, NER, MMR and polymerase components determined by RNAseq analysis in LNCaP cells in standard growth medium (FBS) or in androgen depleted medium, ADT (CS-FBS), or androgen depleted medium supplemented with 10 nM R1881, SPA. **B.** graphical representation of the changes in transcript levels of the repair factors following SPA treatment compared to FBS.

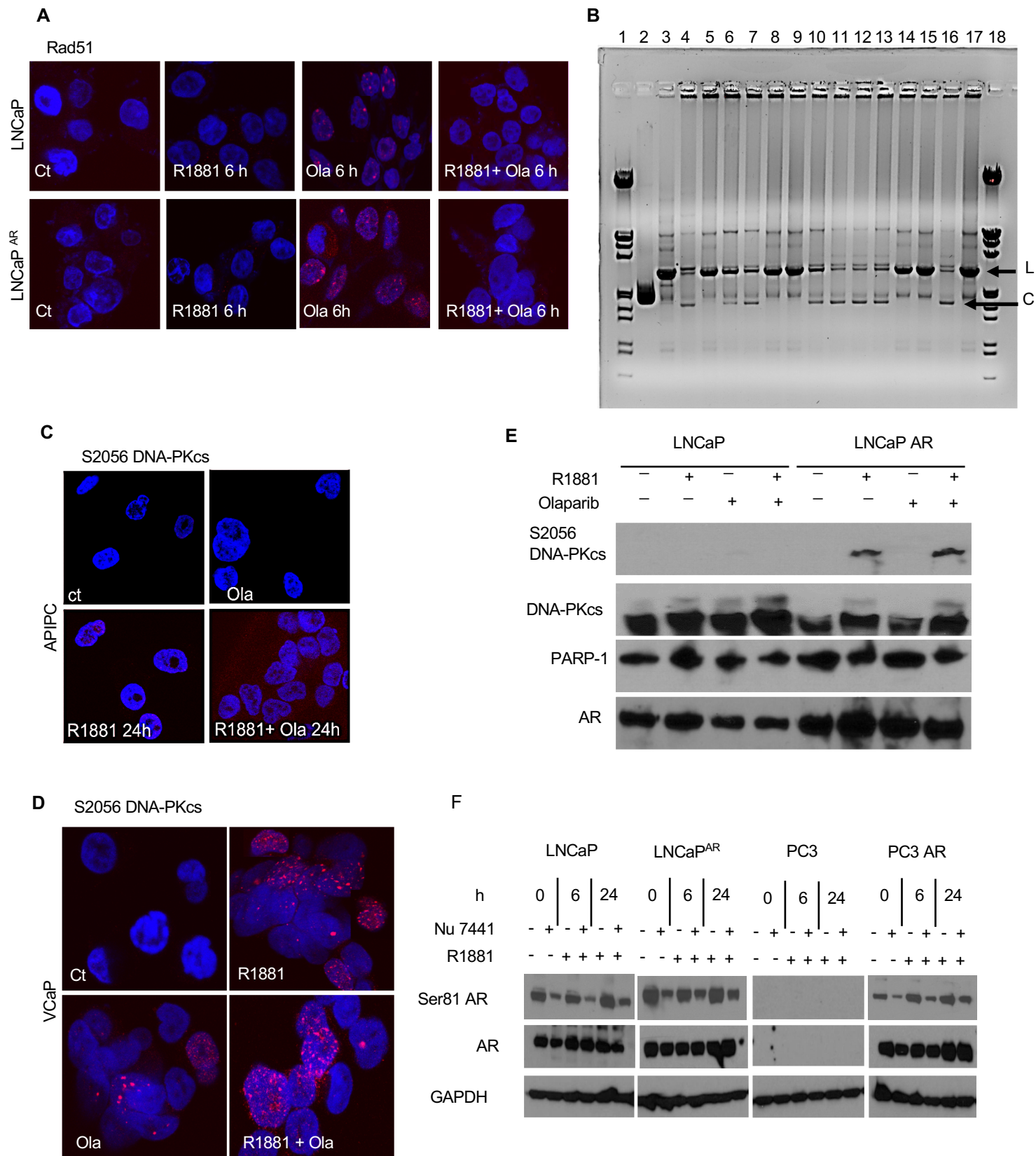


Fig S8: Assessments of HR- and NHEJ-DNA repair pathways following SPA treatment in prostate cancer cells. **(A)** Confocal immunostaining of RAD51, a marker of HR repair in both LNCaP and LNCaP^{AR} cells following SPA alone and Olaparib treatment in combination **(B)** In-vitro DNA end ligation assay, a surrogate experiment to evaluate for NHEJ repair assay using the nuclear extract of all prostate cancer cells LNCaP, LNCaP^{AR} and PC3, PC3^{AR} cells treated with SPA on pUC19 DNA. Lane 1 and 18 are lambda phage markers. Lane 2 is circular pUC19 DNA (C), Lane 3 is EcoR1 restriction digested linearized pUC19 DNA (L), Lane 4-6 are LNCaP cells' nuclear extract treated DNA samples (untreated, 6 and 24h of 10 nM R1881 respectively), Lanes 7-9 are LNCaP^{AR} cells' nuclear extract treated DNA samples (untreated, 6 and 24h of 10 nM R1881 respectively), lanes 10-12 and lanes 13-15 are PC3 and PC3^{AR} cells' nuclear extract treated DNA samples (untreated, 6 and 24h of 10 nM R1881 respectively). Lane 16 is T4 DNA ligase treated pUC19 DNA, used as positive control and lane 17 is pUC19 DNA with no T4 DNA ligase used as negative control. **(C)** Confocal immunostaining of Ser2056 DNA-PKcs foci in LNCaP^{APIPC} cells treated with SPA or olaparib (Ola) or in combination. **(D)** Confocal immunostaining of Ser2056 DNA-PKcs foci in VCaP cells treated with SPA or olaparib or in combination. **(E)** Chromatin fractionation assay in LNCaP and LNCaP^{AR} cells treated with SPA, olaparib and in combination and probed for Ser 2056 DNA-PKcs, DNA-PKcs, PARP-1 and AR. **(F)** Western blot probed for Ser81 AR, AR and GAPDH in LNCaP, LNCaP^{AR} and PC3, PC3^{AR} cells treated with SPA and DNA-PKcs inhibitor NU7441 alone or in combination

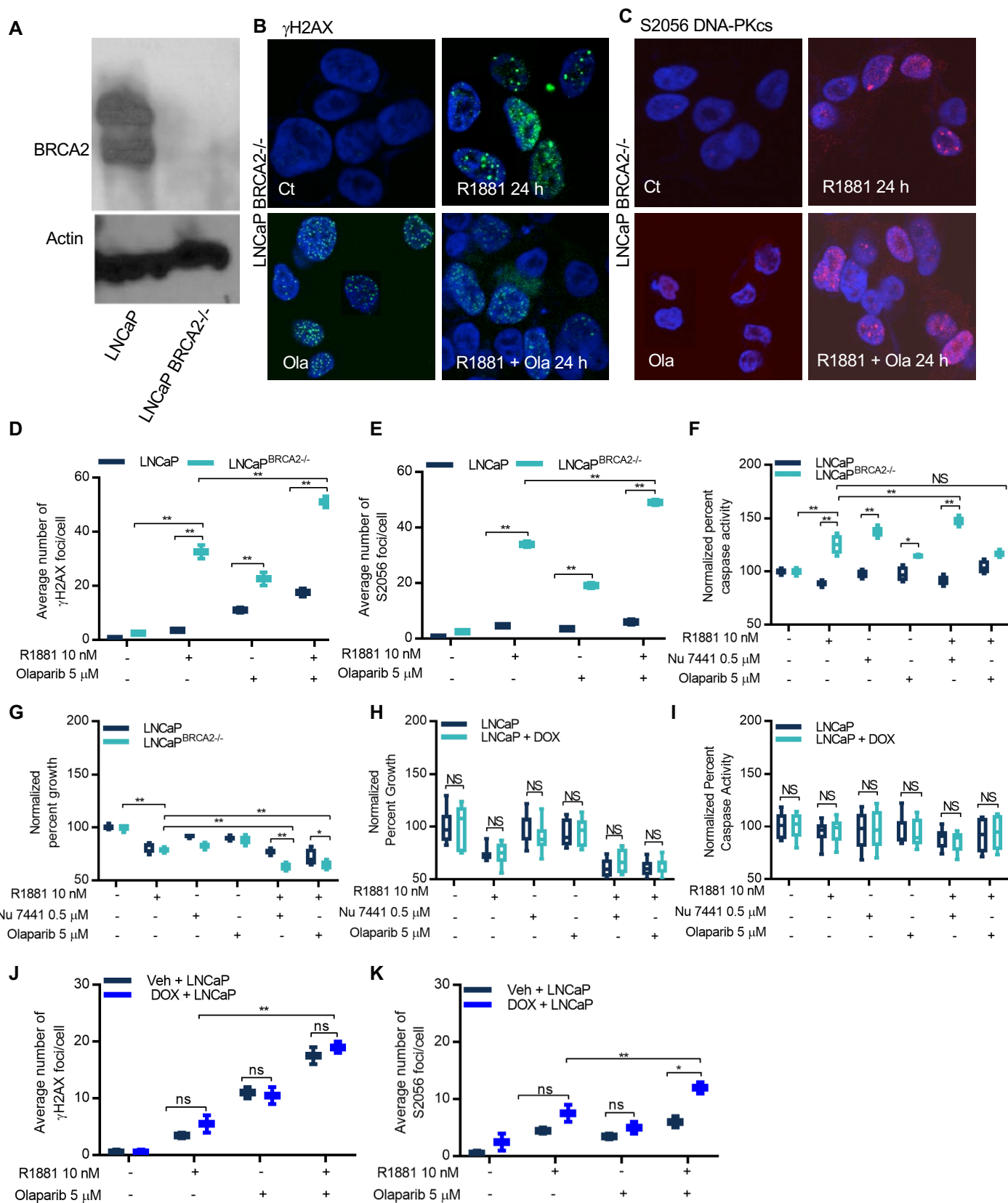


Fig S9. Evaluating the effects of SPA and Olaparib in a LNCaP BRCA2 CRISPR model. **A.** Western immunoblot of BRCA2 protein extracts from LNCaP and LNCaP with CRISPR/Cas9 *BRCA2* gene editing. **B.** Confocal immunostaining and **D.** quantitation of γ H2AX in LNCaP *BRCA2*^{-/-} cells following 10 nM R1881 and/or Olaparib treatment for 24h. **C.** Confocal immunostaining and **E.** quantitation of DNA PKcs S2056 foci in LNCaP *BRCA2*^{-/-} cells following 10 nM R1881 and/or Olaparib treatment for 24h. **F.** Quantitation of apoptosis by caspase activity, and **G.** growth of LNCaP *BRCA2*^{-/-} cells after 3 days treatment with R1881, Nu7441 or Olaparib. **H. and I.** Graphical representation of the estimated growth and caspase activity in LNCaP under the presence or absence of DOX after 3 days treatment with R1881, Nu7441 or Olaparib. **J. and K.** Quantitation of γ H2AX foci and Ser2056foci in LNCaP cells in the presence or absence of DOX following treatment with R1881 or Olaparib. In D, E, F, G, I, J and K data represent mean \pm SD; n=4 replicates per experiment; $p \leq 0.05$ (*), $p < 0.01$ (**) by two-way ANOVA.

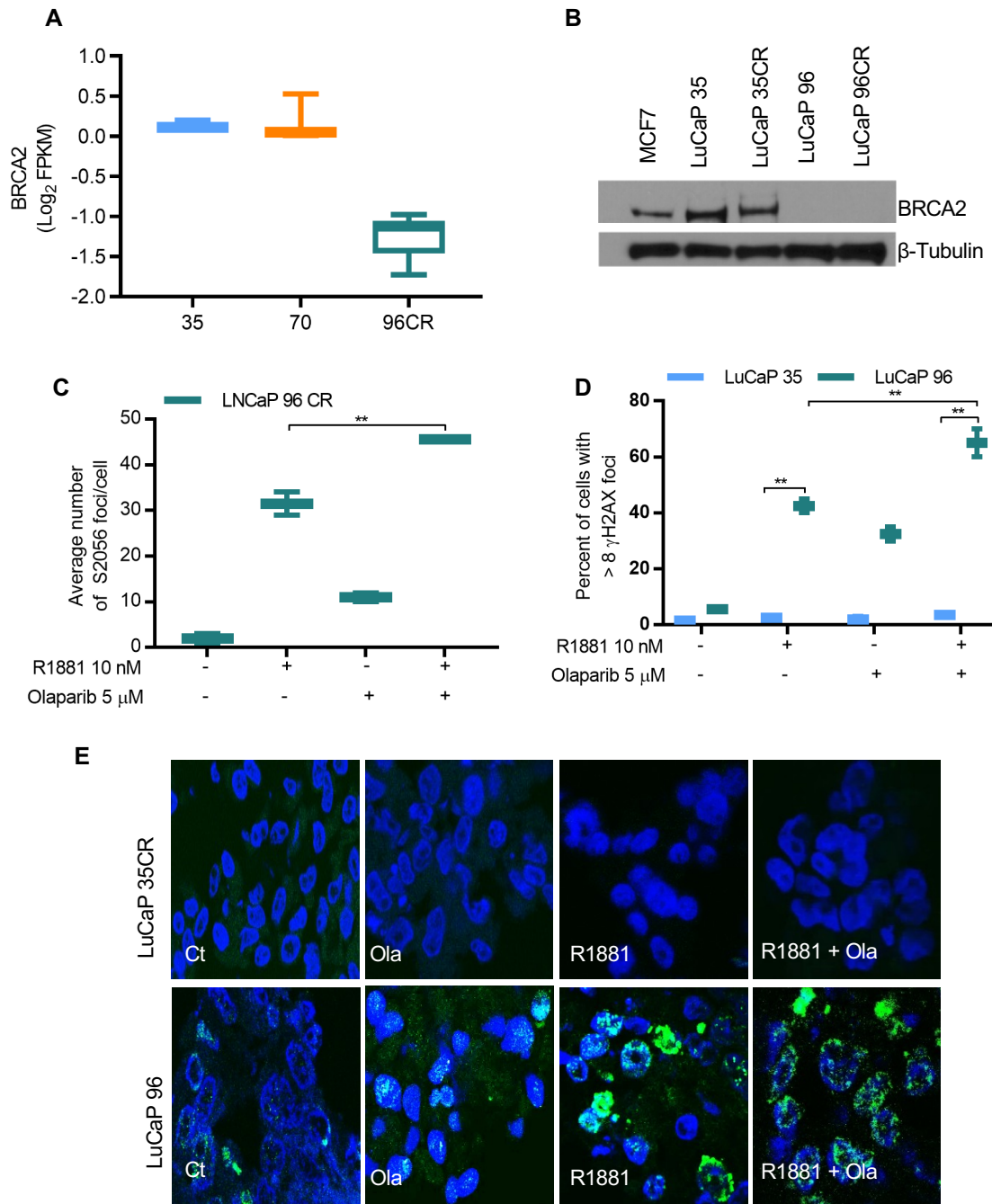


Fig S10. Assessment of the effects of SPA and olaparib in LuCaP PDX models with and without BRCA2 Loss: (A) Transcript levels of BRCA2 in LuCaP 35, LuCaP 70 and LuCaP 96CR PDX tumors determined by RNAseq and plotted as the Log₂ of fragments per kilobase of transcript per million mapped reads (FPKM); (B) Western blot (3-8% Tris-Acetate Gel) probed for BRCA2 protein in MCF7 breast cancer cells as a positive control, and LuCaP 35, LuCaP 35CR, LuCaP 96 and LuCaP 96CR PDX lines. The approximate molecular weight of the BRCA2 band is 400 kDa; (C) Graphs represent the ser2056 DNA-PKcs foci in LuCaP 96CR following R1881 and/or olaparib after 18h exposure; (D) Graphs and (E) confocal immunostaining of γH2AX staining in LuCaP 35CR and LuCaP 96 tissue slice cultures treated *ex-vivo* for 3 days with R1881 and/or olaparib. Data represent the mean ± SD; n=3 replicates per experiment; p≤0.05 (*), p<0.01 (**) by two-way ANOVA.



Table S1. DNA repair gene mutations and PSA responses in men with CRPC enrolled on clinical trials of supraphysiological androgen therapy.

Patient ID	Homologous Recombination (HR) Gene Mutation	HR Mutation	PSA decline from baseline (%)	Sequencing Platform	Specimen Tested
1	BRCA2 S1982Rfs*22	Yes	-100%	Color	Germline DNA
2	BRCA2 p.R2991C	Yes	-99%	PlasmaSELECT	Plasma
3	ATM R2244Kfs*5	Yes	-98%	PlasmaSELECT	Tumor Tissue
4	BRCA2 N319Kfs*8	Yes	-98%	Color	Germline DNA
5	ATM p.V1197Ffs*10	Yes	-91%	UW-OncoPlex	Plasma
6	1) CHD1 copy loss 2) Chromosome 13 copy loss in the region of BRCA2	Yes	-88%	UW-OncoPlex	Plasma
7	1) CDK12 p.G923V mutation and copy neutral LOH 2) BRCA2 p.Y1762* mutation and 1 copy loss	Yes	-84%	UW-OncoPlex	Plasma
8	ATM splicing mutation with LOH	Yes	-78%	UW-OncoPlex	Plasma
9	CHEK2 p.I157T	Yes	-74%	UW-OncoPlex	Plasma
10	CHEK2 p.I157T	Yes	-68%	UW-OncoPlex	Plasma
11	CHD1 copy loss	Yes	-67%	UW-OncoPlex	Plasma
12	1) BRCA1 c.1378_1381del 2) CHEK2 p.I157T 3) CDK12 c.366dup	Yes	-61%	UW-OncoPlex	Plasma
13	PALB2 Q1164*	Yes	-61%	PlasmaSELECT	Tumor Tissue
14	CHEK2 p.L348Kfs*20	Yes	-55%	UW-OncoPlex	Plasma
15	ATM R805*	Yes	-54%	FoundationOne	Tumor Tissue
16	FANCD2 S64Rfs*4	Yes	-44%	FoundationOne	Tumor Tissue
17	PALB2 Q60Rfs*7	Yes	-40%	PlasmaSELECT	Tumor Tissue
18	BRCA2 S1982Rfs*22	Yes	-18%	FoundationOne	Tumor Tissue
19	BRCA2 copy loss	Yes	-11%	SU2C	Tumor Tissue
20	ATM p.Q1627X and p.L2427R	Yes	0%	UW-OncoPlex	Plasma
21	ATM c.8876_8879del	Yes	35%	UW-OncoPlex	Plasma
22	FANCA p.R853*	Yes	37%	UW-OncoPlex	Plasma
23	BRCA2 p.Y1655X mutation and LOH	Yes	130%	UW-OncoPlex	Plasma
24	BRCA2 S2371ks*21	Yes	253%	FoundationOne	Tumor Tissue
25	PALB2 p.W1038X	Yes	310%	UW-OncoPlex	Plasma
26	BRCA2 p.Y2977Ffs*11	Yes	353%	UW-OncoPlex	Plasma
27	CHEK2 p.L348Kfs*20	Yes	513%	Color	Germline DNA
28	CDK12 c.1995dup	Yes	603%	UW-OncoPlex	Plasma
29	ATM p.Q284X*	Yes	662%	PlasmaSELECT	Plasma
30		No	-94%	UW-OncoPlex	Tumor Tissue
31		No	-85%	UW-OncoPlex	Tumor Tissue
32		No	-72%	UW-OncoPlex	Plasma
33		No	-66%	UW-OncoPlex	Plasma

34		No	-63%	FoundationOne	Tumor Tissue
35		No	-51%	UW-OncoPlex	Plasma
36		No	-48%	FoundationOne	Tumor Tissue
37		No	-38%	PlasmaSELECT	Tumor Tissue
38		No	-36%	UW-OncoPlex	Plasma
39		No	-35%	UW-OncoPlex	Plasma
40		No	-11%	UW-OncoPlex	Plasma
41		No	-8%	UW-OncoPlex	Plasma
42		No	13%	UW-OncoPlex	Plasma
43		No	22%	UW-OncoPlex	Plasma
44		No	26%	UW-OncoPlex	Plasma
45		No	28%	Guardant360	Plasma
46		No	28%	UW-OncoPlex	Plasma
47		No	49%	UW-OncoPlex	Plasma
48		No	65%	UW-OncoPlex	Plasma
49		No	81%	UW-OncoPlex	Plasma
50		No	83%	FoundationOne	Tumor Tissue
51		No	122%	UW-OncoPlex	Plasma
52		No	135%	PlasmaSELECT	Tumor Tissue
53		No	144%	UW-OncoPlex	Plasma
54		No	154%	FoundationOne	Tumor Tissue
55		No	158%	PlasmaSELECT	Plasma
56		No	424%	UW-OncoPlex	Plasma
57		No	494%	FoundationOne	Tumor Tissue
58		No	514%	UW-OncoPlex	Plasma
59		No	529%	FoundationOne	Tumor Tissue
60		No	785%	PlasmaSELECT	Plasma
61		No	2027%	PlasmaSELECT	Tumor Tissue
62		No	2147%	FoundationOne	Tumor Tissue